WILEY | Hindawi

Research Article

Effect of *Cycas pectinata* Seed Extract on Testicular Steroidogenesis in a Mouse Model

Chuckles Ch. Marak [ID],[1] **Brilliant N. Marak** [ID],[2] **Ved Prakash Singh** [ID],[2] **Guruswami Gurusubramanian** [ID],[1] and **Vikas Kumar Roy** [ID][1]

[1]*Department of Zoology, Mizoram University, Aizawl, Mizoram 796 004, India*
[2]*Department of Industrial Chemistry, Mizoram University, Aizawl, Mizoram 796 004, India*

Correspondence should be addressed to Vikas Kumar Roy; vikasroy4araria@yahoo.co.in

The seed of *Cycas pectinata* is widely used in traditional practices in the Northeastern region of India for diverse purposes along with improving testicular functions. Thus, it may be hypothesized that the phytochemicals of *C. pectinata* seed could modulate testicular steroidogenesis. Therefore, we have investigated the effects of *C. Pectinata* seed extract (CPE) on testicular steroidogenesis by using *in vivo* and *in vitro* approaches. We have also performed the molecular docking of phytochemicals with some steroidogenic markers based on the identified phytochemicals from our previous study. The *in vivo* treatment of CPE increased the circulating estrogen and decreased circulating testosterone. The *in vitro* treatment of CPE also showed increased secretion of estrogen which can be suggested due to an increase in the aromatase (CYP19A1) activity. Our results also showed that the expression and localization of CYP19A1 were elevated by the CPE. The treatment of CPE also showed an accumulation of cholesterol in the testis, which could enhance testicular steroidogenesis. The other steroidogenic markers like 3βHSD, StAR, and LHR were upregulated by the CPE. Twelve compounds exhibited binding energy in the range of -10.0 to -8.0 kcal/mol with CYP19A1. Our data from *in vitro*, *in vivo*, and docking studies, showed that phytochemicals of CPE could modulate testicular steroidogenesis.

1. Introduction

Plants and their important constituents have been extensively used as sources of drugs and therapeutic agents and broadly have been using in medication in the developing world [1]. About 80% of people depend on herbal products as per the report given by World Health Organization for their primary health care [2]. *Cycas pectinata* Buch.-Ham are tall, evergreen, and palm-like trees [3]. Different parts of *C. pectinata* are eaten as vegetables by local communities and also used as traditional medicines in many cultures as it has various ethnomedicinal uses and pharmacological effects [4, 5], while some local Indian communities in Meghalaya and Assam use seeds of *C. pectinata* as a source of starch and also to boost male fertility [3]. This information was collected from the local people and traditional practitioners of herbal drugs in Meghalaya. Some studies

have also shown that the methanolic extract of *C. pectinata* leaves showed antioxidant, anti-inflammatory, and analgesic properties [5] whereas *C. pectinata* fruit extract possesses antidiabetic properties, having amentoflavone and 2,3-dihydroamentoflavone [4]. In a recent study, we have shown that crude seed extract of *C. pectinata* has a variety of phytochemical compounds (32 phytochemicals) with certain biological activities [6].

Based on the information collected from the local people and traditional practitioners of herbal drugs, it could be suggested that the seed of *C. pectinata* might influence testicular steroid production via modulating Leydig cell steroidogenic pathways. Our recent report on seed extract of *C. pectinata* suggested some biological functions of the extract such as antioxidant, antineoplastic activity, and most importantly, the cholesterol antagonist activity and agonist of testosterone 17β-dehydrogenase, which plays a major role in steroid

TABLE 1: Binding affinity and the residues involved in the interaction of phytochemical compounds with CYP19A1.

Compounds	Binding affininity (kcal/Mol)	Residues involved in H-bond	Residues involved in other interactions (π-alkyl and alkyl)
3-Didehydro-5-dehydroxyhydratoperidinin	-10.1	Cys437, Ala438	Ile132, Ile133, Phe134, Phe138, Leu152, Phe221, Val370, Val373
6-Epiheteroxanthin	-8.7		Ile133, Phe134, Phe221, Trp224, Ile305, Ala306, Val364, Val369, Val370, Leu372, Met374, Phe430, Cys437, Ala438, Ala443, Leu477
Astaxanthin	-9.9	Arg115, Arg145, Thr310, Ser314	Ile133, Trp224, Met364, Val369, Val370, Phe430, Ala306, Cys437, Ala438
Auroxanthin	-8.2	Ala438, Gly439	Ile132, Ile133, Phe148, Leu152, Phe221, Met303, Ala306, Val370, Val373, Cys437, Leu477
Corbiculaxanthin	-9.8	Arg145, Thr310	Ile133, Phe148, Phe221, Trp224, Ile305, Ala306, Met364, Val369, Val370, Val373, Phe430, Cys437, Ala438
Cucurbitaxanthin_A	-9.2		Ile132, Ile133, Phe134, Leu152, Phe221, Trp224, Ala306, Val370, Phe430, Cys437, Ala438, Leu477
Cycloviolaxanthin	-8.3		Ile132, Ile133, Phe134, Phe148, Leu152, Trp224, Met303, Ile305, Ala306, Met364, Val369, Val370, Phe430, Cys437, Ala438
Halocynthiaxanthin	-9.3	Ala306	Ile133, Phe148, Phe221, Met364, Val370, Val373, Phe430, Cys437, Ala438
Ipomoeaxanthin_A	-9.3	Ser314, Cys437	Ile132, Ile133, Phe148, Leu152, Trp224, Ala306, Met364, Val369 Val370, Val373, Ala438, Phe430
Mactraxanthin	-9.5	Cys437	Ile133, Phe134, Phe221, Ala306, Ala307, Val370, Val373, Met374, Phe430, Leu477
Pyrrhoxanthinol	-9.7	Arg115, Leu372, Pro429	Ile305, Ile306, Phe134, Phe148, Leu152, Phe221, Trp224, Val370, Val373, Cys437, Ala438, Leu477
Pyrrhoxathinol 5,8-furanoide	-9.2	Arg115, Arg145, Ala438	Ile132, Ile133, Phe148, Phe221, Trp224, Ala306, Val370, Gly436, Cys437

biosynthetic pathways [6]. To the best of our knowledge, there is no report on the effect of *C. pectinata* on steroidogenic activity. It is well known that Leydig cells possess steroidogenic enzymes capable of producing various androgens via a process called steroidogenesis [7]. Androgens such as androstenedione and testosterone are cholesterol derivatives, which regulate testicular development, and differentiation of the male [8]. Leydig cells carried out the steroidogenic activity through a network of proteins, mediating cholesterol delivery to CYP11A1 [9]. Testicular steroidogenesis also involves the synthesis of estrogen from testosterone via aromatase (CYP19A1) [10]. The overall pathways of Leydig cell steroidogenesis consist of the transfer of cholesterol to mitochondria by steroidogenic acute regulatory protein (StAR) and further processing by 3β hydroxysteroid dehydrogenases (3βHSD) and 17β hydroxysteroid dehydrogenases (17βHSD) and CYP19A1 [11, 12].

Based on the above information, we hypothesized that the phytochemical seed extract of CPE could modulate the steroid production by affecting the different steroidogenic factors such as 3βHSD and 17βHSD, CYP19A1, and steroidogenic acute regulatory protein (StAR). Therefore, the present study is aimed at investigating the effects of CPE on testicular steroid production by *in vivo* and *in vitro* approaches along with the possible interaction of different phytochemicals of CPE with markers of steroidogenesis utilizing molecular docking study.

2. Materials and Methods

2.1. Plant Material and Preparation of Extract. The seeds of *C. pectinata* were collected from West Garo Hills, Meghalaya, India, in August 2019. A voucher specimen (BSI/ERC/Tech/2020/1309) was deposited and accession number 96583 was obtained from the Botanical Survey of India, Shillong.

Cycas pectinata seed extract (CPE) was prepared following the method described earlier [6]. Briefly, fresh seeds of *C. pectinata* were washed with water, chopped into pieces, dried at room temperature, and powdered using an electrical blender. Briefly, 100 g of *C. pectinata* seed powder was added to 500 ml of methanol on a clean beaker and soaked for 3 days by occasional shaking and stirring at room temperature. The extract was filtered using Whatman filter paper (Grade 1

3-Didehydro-5-dehydroxyhydratoperidinin

(a)

Hupehemonoside

(b)

Corbiculaxanthin

(c)

Pseudojervine

(d)

Astaxanthin

(e)

Cyclogaleginoside A
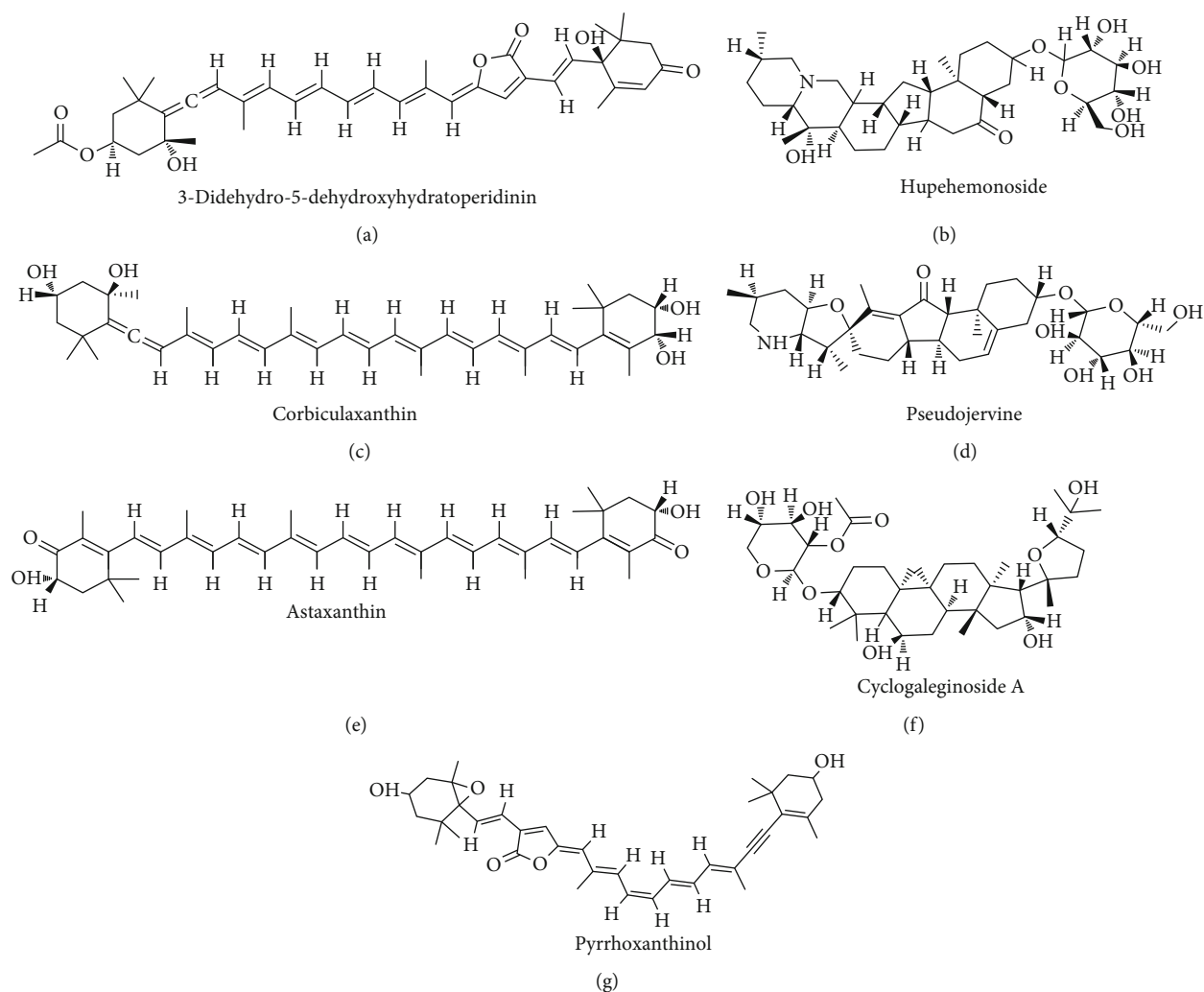
(f)

Pyrrhoxanthinol

(g)

Figure 1: Structures of phytochemicals. 3-Didehydro-5-dehydroxyhydratoperidinin (a). Hupehemonoside (b). Corbiculaxanthin (c). Pseudojervine (d). Astaxanthin (E cyclogaleginoside A (f). Pyrrhoxathinol (g).

circles—150 mm), and the obtained filtrate was evaporated to yield a viscous mass and stored at 4°C for further use.

2.2. Molecular Docking. Molecular docking calculations were carried out using AutoDock Vina. The 3D X-ray crystal structures of CYP19A1, CYP11A1, and 17βHSD were obtained from the RSCB protein data bank (PDB id: 5JKW, 3N9Y, and 1DHT). Before docking, the proteins are prepared by removing water molecules, cofactors, and cocrystallized ligands attached to the protein. The polar hydrogens are then added to the protein in AutoDock tools and saved in pdbqt format. The 3D structures of phytochemicals that were identified through LC-MS were created in ChemDraw, and the energy is optimized using the MMFF94 force field. The grid parameters for docking in the active site of CYP19A1, CYP11A1, and 17βHSD were assigned based on the native ligand testosterone, cholesterol and 5-alpha-dihydrotestosterone, respectively, ensuring all the residues in the binding pocket are covered. The exhaustiveness parameter was set to 8 modes, and the phytochemical compounds were subjected to docking using AutoDock

Vina. Finally, Pymol and Discovery Studio were used for the visualization of docking poses.

2.3. Experimental Animals: In Vivo Study. Swiss albino male mice (3 months old) weighing 30-35 g were used for investigations. Mice were kept in an aerated polypropylene cage with ad libitum access to food and water at $22 \pm 3°C$ temperature under a 12/12 h light/dark cycle. All experimental procedures were conducted in compliance with the protocols approved by the Mizoram University Institutional Animal Ethical Committee (approval no. MZU/IAEC/2020/06) under CPCSEA guidelines.

Male mice ($n = 15$) were randomly allocated to three groups of five animals each, the extract was suspended in sterile distilled water and administered orally with the help of an oral gavage: Group I, distilled water-treated control and Groups II and III, administration of CPE 100 and 400 mg/kg of body weight, respectively, which was considered to be the safest dose as per the subacute toxicity test based on our previous study [6]. The treatment duration was for 35 days because the duration of one spermatogenic
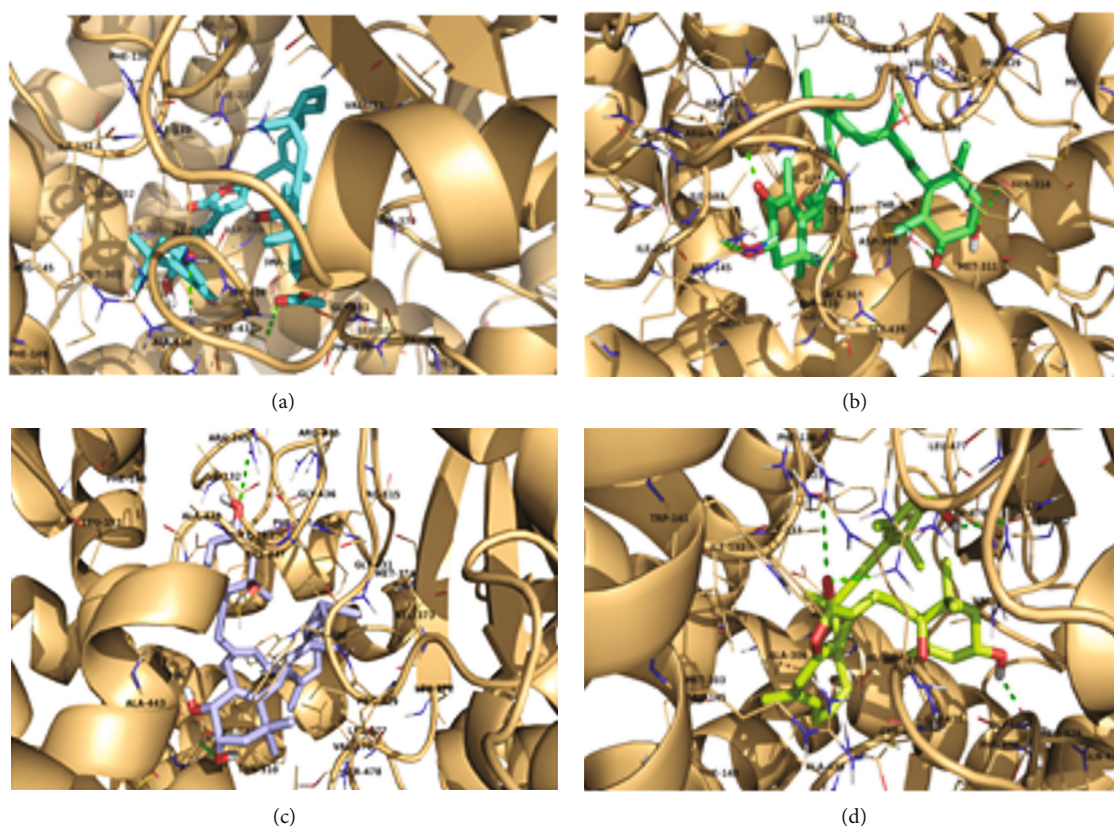
Figure 2: 3D structure for molecular interactions of the docked compounds with CPY19A1. Depiction of binding mode of phytochemicals in the active site of CYP19A. (a) 3-Didehydro-5-dehydroxyhydratoperidinin. (b) Astaxanthin. (c) Corbiculaxanthin. (d) Pyrrhoxanthinol.

cycle is 35 days in mice. Mice were sacrificed under mild anesthesia (i.p. injection of ketamine and xylazine 90 : 10 mg/kg, respectively) on the 36th day after 24 hours of the last oral treatment. Testis was collected and blood serum was separated for biochemical parameters and stored at -20°C until further use.

2.4. Immunohistochemistry and Quantification by ImageJ. For evaluation of steroidogenic activity, the testis of each mouse was excised from each group, fixed in Bouin's fluid, dehydrated in graded ethanol series (i.e., 70%, 90%, and 100%, respectively) cleared in xylene and embedded in paraffin. Tissues were sectioned at $7\,\mu m$ thickness using Leica rotary microtome (model RM2125 RTS), and using sterile glass slides, the tissue sections were attached. The slides were then deparaffinized with xylene followed by rehydration using graded series of ethanol solutions of decreasing concentrations, i.e., 100%, 90%, and 70% for 10 minutes each and processed for immunohistochemistry using 3βHSD (1 : 200, Santa Cruz Biotech. Cat# Sc-515120 HRP lot #J1117), 17βHSD (1 : 400, St. John's lab cat# STJ110000), aromatase or CYP19A1 (1 : 200, St. John's lab cat# STJ110000), StAR (1 : 200, St. John's lab cat# STJ191473), and LHR (1 : 200, Santa Cruz Biotechnology Sc-25828 Lot# B1213). The unbound primary antibody was washed off by phosphate buffer saline (PBS) solution and incubated with horseradish peroxidase- (HRP-) conjugated secondary IgG anti-

body 1 : 400 dilution (goat anti-rabbit, cat# PI-1000, Vector Laboratories, Burlingame, CA, US) for 4 h at room temperature. Unbound antibodies were washed off with PBS and incubated in a solution containing 0.6 mg/ml solution of 3,3-diaminobenzidine tetrahydrochloride dihydrate (DAB) in Tris-HCL (pH 7.6) and 0.01% H_2O_2 till brown color develops. The reaction was stopped in distilled water for 10 minutes and counterstained with hematoxylin followed by dehydration. The slides were then cleared in xylene, and DPX was used for mounting. The negative control slides were also processed with 1% mouse nonimmune IgG for 3βHSD and 1% rabbit nonimmune IgG for 17βHSD, CYP19A1, StAR, and LHR to check the specificity of the primary antibody. Immunostaining of the slides was assessed under a Nikon microscope (Model E200, Nikon, Tokyo, Japan) and photographed.

The semiquantification of 3βHSD, 17βHSD, CYP19A1, StAR, and LHR staining in the testes of the control and treatment was executed by ImageJ software. The stained area by DAB in the testis was acquired by using the threshold tool of ImageJ as described by [13], and the data were presented as a percentage area of staining. In brief, the image was opened in ImageJ and the color deconvolution2 plugin tool was selected followed by H and E DAB vector (image were kept in 8-bit transmittance), resulting in three images; the DAB stained image was selected and percentage area was obtained by selecting "Image–Adjust–Threshold." After selecting the threshold, the sliders in the pop-up window were manually

TABLE 2: Binding affininity and the residues involved in the interaction of phytochemical compounds with CYP11A1.

| Compounds	Binding affinity (kcal/mol)	Residues involved in H-bond	Residues involved in other interactions (π-alkyl and alkyl)
Hupehemonoside	-10.7	Asn210, Gln377, Val353	Leu460, Ile84, Leu101
Pyrrhoxanthinol	-10.4	Arg81	Ile84, Val101, Leu209, Val353, Phe548, Leu460, Ile461, Lue355
Pseudojervine	-10.3	Asn210, Arg81	Leu209, Phe82, Phe548, Val353, Leu460
Cyclogaleginoside A	-10.3	Phe82	Leu209, Phe548, Val353, Leu460, Trp87, Ile84, Phe82
Cyclopyrroxanthin	-10.0	Glu283	Leu101, Leu424, Leu209, Phe548, Val353, Val35, His29, Ile84, Phe82, cys423
Pyrrhoxathinol 5,8-furanoide	-9.6		Arg81, Phe82, Leu101, Leu424, Leu209, Phe548, Met284, His39, Val100, Val35, cys423, Val353, Val57, Ile84
3-Didehydro-5-dehydroxyhydratoperidinin	-9.1		Leu101, Leu424, Met284, Cys423, Ile84, Leu209, Val353

(a)

(b)

(c)

(d)
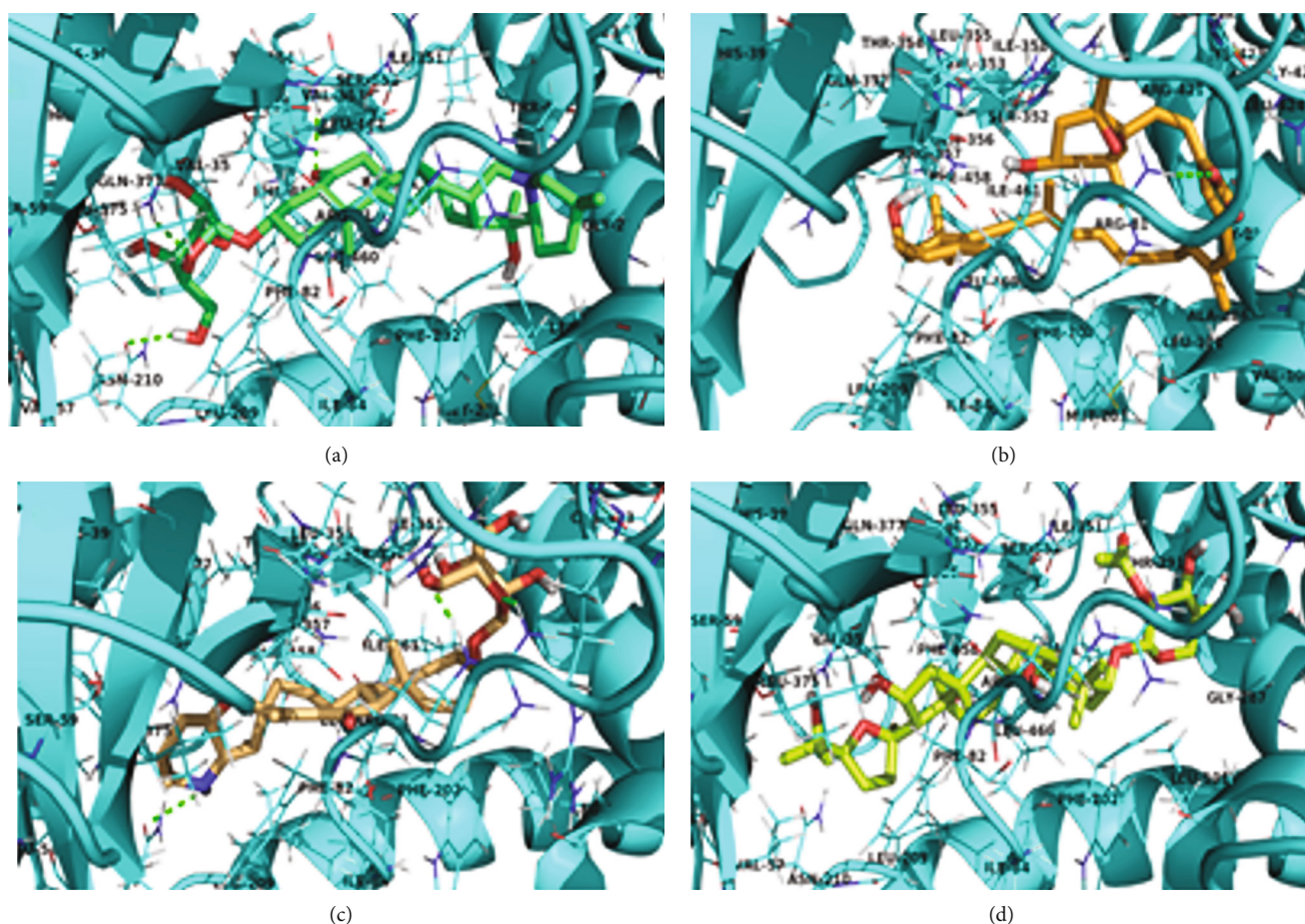
FIGURE 3: 3D structure for molecular interactions of the docked compounds with CYP11A1. Depiction of binding mode of phytochemicals in the active site of CYP11A1. (a) Hupehemonoside. (b) Pyrrhoxanthinol. (c) Pseudojervine. (d) Cyclogaleginoside A.

moved to get the stained area. Then, it was clicked on apply followed by a selection of analyze–set measurements. The limit to threshold, area, and area fraction options was selected. The percentage stained area was obtained by selecting analyze and measure from the menu of ImageJ.

2.5. Biochemical Assay. The blood was collected in the tubes and centrifuged at 12,000 rpm for 15 min. The serum from each sample was collected and stored at -80°C for biochemical assay. Biochemical assay viz. cholesterol (Euro diagnostic system #Lot OL04758), high-

TABLE 3: Binding affinity and the residues involved in the interaction of phytochemical compounds with 17βHSD.

Compounds	Binding affininity (kcal/mol)	Residues involved in H-bond	Residues involved in other interactions (π-alkyl and alkyl)
Hupehemonoside	-9.3		Phe259, Val225, Pro187, Phe226, Met193
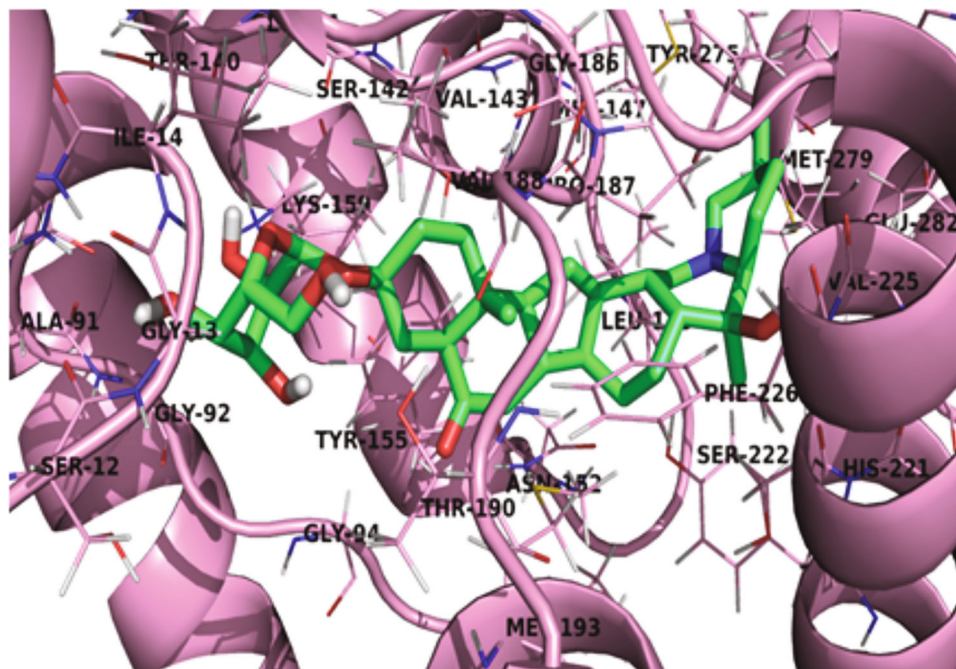
FIGURE 4: 3D structure for molecular interactions of the docked compounds with 17βHSD. Depiction of binding mode of phytochemicals in the active site of 17βHSD. Hupehemonoside with 17βHSD.

density lipoprotein or HDL (Euro diagnostic system #Lot EHD-09/1219), and low-density lipoprotein or LDL (Coral clinical system, #cat 1102160025) were done at the end of the experiment by using the commercial kit as per the kit's instructions.

To estimate the testicular cholesterol, a 10% testis sample was homogenized with phosphate buffer saline and centrifuge at 12,000 rpm for 15 min, thereafter, supernatant was collected and cholesterol (Euro diagnostic system #Lot OL04758) was estimated using a commercially available kit as per the kit's instructions.

2.6. Hormonal Assay.
Serum level concentration such as testosterone (cat# EIA 100-03, Alkor Bio Company Ltd.), estrogen (cat# DKO003, DiaMetra, Italy), and androstenedione (cat# DIA DKO008, DiaMetra, Italy) was measured by the ELISA method by using a commercial kit according to the manufacturer's instruction. The absorbance reading was taken at 450 nm using a microplate ELISA reader (Erba Lisa Scan EM, Trans Asia Biomedical Ltd, Mumbai, Maharashtra, India).

2.7. Western Blotting.
Western blotting of steroidogenic markers in the testis was performed by following the standard protocol of Jeremy et al. [14]. The collected mice testes were pooled separately from each group and homogenized

in suspension buffer 0.01 M Tris pH 7.6, 0.1 M EDTA (pH 8.0), 0.1 M NaCl, 1 mg/ml aprotinin, and 100 μg/ml phenylmethylsulfonyl fluoride (PMSF) in a glass homogenizer to produce 10% (w/v) homogenate. An equal amount (50 μg) of protein from each group was loaded to each well along with a molecular weight marker in a 12% sodium dodecyl sulfate-polyacrylamide gel electrophoresis (SDS-PAGE–12% gel, HiMedia, Mumbai, India) for electrophoresis. Thereafter, proteins were transferred electrophoretically to polyvinylidene fluoride membrane (Millipore India Pvt. Ltd., Bangalore, India) for 14 h at 4°C. Membranes were blocked for 30 min with Tris-buffered saline (TBS; Tris 50 mM (pH 7.5), NaCl 150 mM, 0.02% Tween 20) containing 5% fat-free dry milk and incubated with primary antibody aromatase (1 : 2500, Elabscience cat# E-AB-64300), 17βHSD (1 : 3000, St. John's lab cat# STJ110000), StAR (1 : 2000, St. John's lab cat# STJ191473), and P450 (1 : 1000, Bioss cat# Bs-3608R) for overnight at 4°C. Membranes were then washed with four changes with PBST for 15 mins. Immunoreactive bands were detected by incubating the membranes with horse radish peroxidase- (HRP-) conjugated goat anti-rabbit secondary antibody (dilution 1 : 4000; Elabscience cat# E-AB-1102) for 4 hours at room temperature. Finally, the blot was washed four times with PBST and developed with enhanced chemiluminescence (ECL) detection system (Cat#-K820, Biovision, Milpitas, CA). The membranes
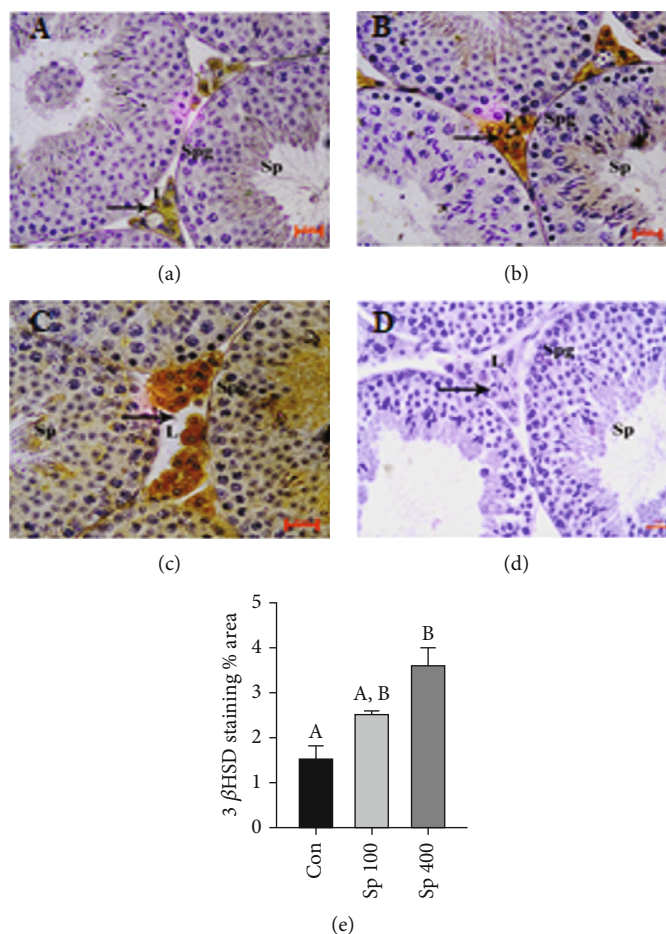
(a)

(b)

(c)

(d)

(e)

FIGURE 5: Abundance of 3βHSD in the testis after CPE treatment. The intense immunostaining of 3βHSD shown in the Leydig cells of 100 mg/kg (b) and 400 mg/kg (c) CPE-treated testis, whereas control showed mild immunostaining (a). The negative control section showed no immunostaining of 3βHSD (d). The quantification 3βHSD-stained area showed a significant ($p < 0.05$) increase in the staining area in the 400 mg/kg-treated group compared to the control and 100 mg/kg groups (e). Data are expressed as mean ± SEM. Different alphabet letters above the bar graph indicate statistically significant differences between groups.

were stripped and reprobed for β-tubulin (1 : 1500 cat #E7; DSHB, University of Iowa, Department of Biology, United States) as a loading control and secondary antibody (1 : 4000, Goat anti-mouse, cat# E-AB1001, Elabscience, Houston, Texas, United States). Densitometric analysis of the blots was performed by scanning and quantifying the bands for density value by using computer-assisted image analysis (ImageJ 1.38x, NIH, Bethesda, MD). The densitometric data were presented as the mean of the integrated density value ± SEM.

2.8. In Vitro Study. In vitro experiment was conducted to study the effect of C. pectinata on testosterone, estrogen, and androstenedione secretion. The mice were sacrificed after mild anesthesia, and the testes were taken out. The testes were cut into equal pieces, and testis explant cultures were performed. Further, the testis explants were cultured for 24 hrs according to the method described by Jeremy et al. [14]. In brief, the testes were cut into equal fragments and weighed 10 mg then adhering tissue was cleaned and cultured in the presence of CPE 1 μg/ml, 10 μg/ml, 100 μg/ml, and con (Without CPE) in a DMEM: Ham'F12 medium (1 : 1) with penicillin (100 U/ml) and streptomycin (100 μg/

ml) in a humidified atmosphere with 95% air and 5% CO_2 to maintain pH 7.4 for 24 h at 37°C. After 24 h, the media were harvested for hormonal assays such as testosterone (cat# EIA 100-03, Alkor Bio Company Ltd.), estrogen (cat# DKO003, DiaMetra, Italy), and androstenedione (cat# DIA DKO008, DiaMetra, Italy) secretion.

2.9. Statistics. All results were expressed as mean (±) standard error of the mean (SEM). Statistical significance was set at $p < 0.05$. Statistical analysis was performed by one-way ANOVA to compare means, and significant differences were further analyzed by Tukey's multiple comparisons using GraphPad Prism (version 9, GraphPad Software, La Jolla, CA).

3. Results

3.1. Docking of Phytochemicals with CYP19A1. Based on the binding affinities of the phytochemicals with CYP19A1, twelve compounds (3-didehydro-5-dehydroxyhydratoperidinin, 6 epiheteroxanthin, astaxanthin, auroxanthin, corbiculaxanthin, cucurbitaxanthin A, cycloviolaxanthin, halocynthiaxanthin, ipomoeaxanthin A, mactraxanthin, pyrrhoxanthinol, and
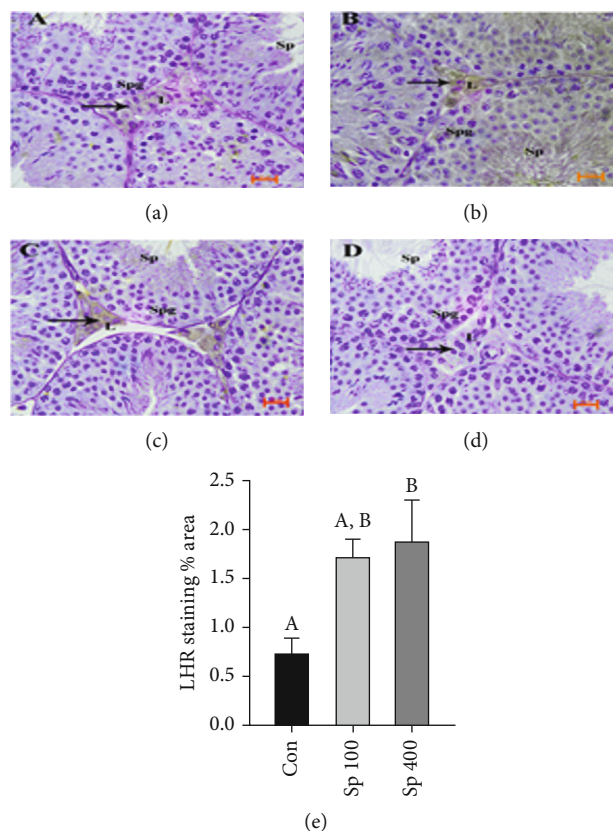
(a)

(b)

(c)

(d)

(e)

FIGURE 6: Abundance of LHR in the testis after CPE treatment. The moderate immunostaining of LHR shown in the Leydig cells of 100 mg/kg (b) and 400 mg/kg (c) CPE-treated testis, whereas control showed mild immunostaining (a). The negative control section showed no immunostaining of LHR (d). The quantification LHR stained area showed a significant ($p < 0.05$) increase in the staining area in the 400 mg/kg-treated group compared to the control and 100 mg/kg groups (e). Data are expressed as mean ± SEM. Different alphabet letters above the bar graph indicate statistically significant differences between groups.

pyrrhoxathinol 5,8-furanoide) that exhibited the binding energy in the range of -10.0 to -8.0 kcal/mol were identified (Table 1). The chemical structures of these compounds are shown in Figure 1. These phytochemicals are stabilized in the binding cavity of CYP19A1 predominantly by hydrogen bonds and hydrophobic π-alkyl and alkyl weak noncovalent interactions (Figures 2(a)–2(d)).

3.2. Docking of Phytochemicals with CYP11A1.
Hupehemonoside, pyrrhoxanthinol, pseudojervine, cyclogaleginoside A, cyclopyrroxanthin, pyrrhoxathinol 5,8-furanoide, and 3-didehydro-5-dehydroxyhydratoperidinin showed binding with CYP11A1 (Table 2). Further, it is stabilized by alkyl interactions with the residues Ile84, Leu101, and Leu460. Pyrrhoxanthinol and cyclopyrroxanthin exhibited one hydrogen bond interaction each with Arg81 and Glu283, respectively, while pseudojervine formed two hydrogen bonds with Arg81 and one with Asn210 (Figures 3(b)–3(d)). The hydrogen bond interactions being absent, the stability of cyclogaleginoside A, pyrrhoxathinol 5,8-furanoide, and 3-didehydro-5-dehydroxyhydratoperidinin are mainly reinforced by the extensive π-alkyl and alkyl interactions (Table 2). It was observed that only hupehemonoside showed the highest binding with CYP11A1 (-10.7 kcal/mol). Hupehemonoside exhibited three hydrogen

bonds with the side chain residues Asn210, Val353, and Gln377 (Figure 3(a)).

3.3. Docking of Phytochemicals with 17βHSD.
The docking analysis has shown that phytochemicals have a less binding affinity towards 17βHSD. Only hupehemonoside showed a binding affinity with 17βHSD (-9.3 kcal/mol). Hupehemonoside is also stabilized by only π-alkyl and alkyl interactions with the residues Pro187, Met193, Val225, Phe226, and Phe259 in the active site of 17βHSD (Table 3). The binding of hupehemonoside has shown with 17βHSD (Figure 4). The chemical structure of compounds has been given in Figures 1(a)–4(g).

3.4. Effect of CPE on the Localization of 3βHSD Protein.
To analyze the possible involvement of CPE on testicular steroidogenesis, localization of 3βHSD was performed. 3βHSD was localized in the Leydig cells (Figures 5(a)–5(d)). The semiquantification of 3βHSD staining showed a significantly ($p < 0.05$) highest abundance in the Leydig cells of mice testis treated with 400 mg/kg of CPE compared to the control and 100 mg/kg CPE groups (Figure 5(e)). The abundance of 3βHSD was also increased in the 100 mg/kg-treated group compared to the control.
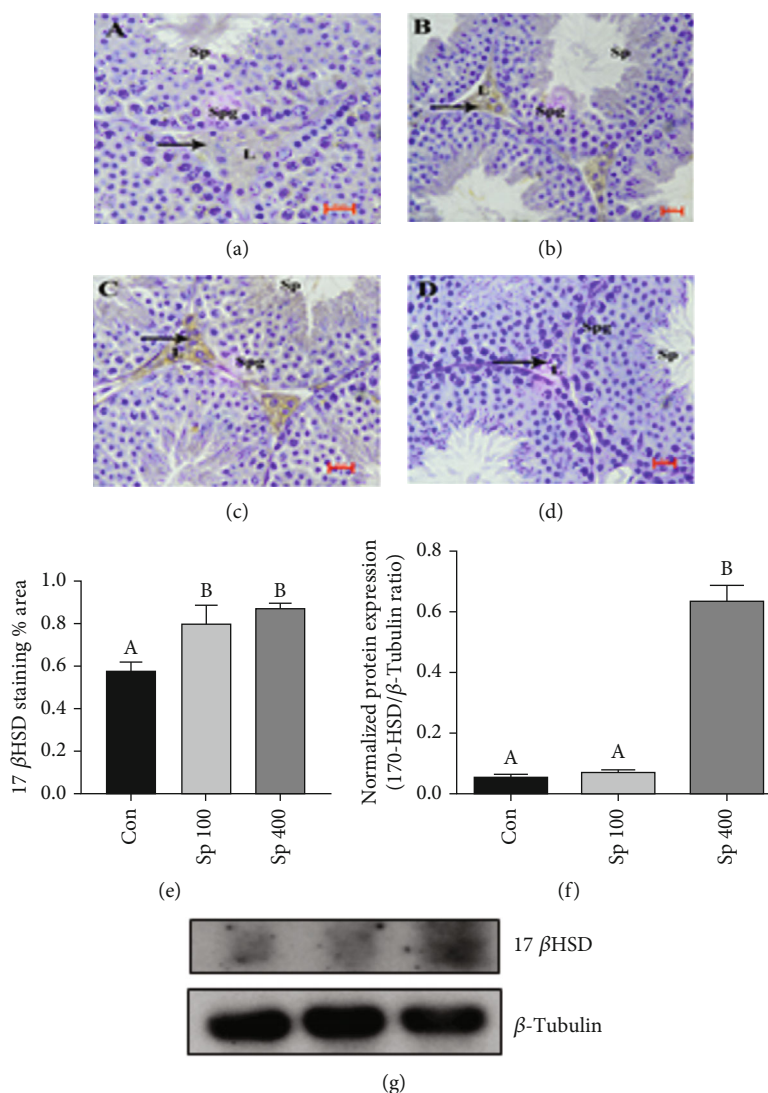
(a)

(b)

(c)

(d)

(e)

(f)

(g)

FIGURE 7: Localization and expression of 17 βHSD in the testis after CPE treatment. The moderate immunostaining of 17 βHSD shown in the Leydig cells of 100 mg/kg (b) and 400 mg/kg (c) CPE-treated testis, whereas control showed mild immunostaining (a). The negative control section showed no immunostaining of 17 βHSD (d). The quantification of 17 βHSD-stained area showed a significant ($p < 0.05$) increase in the staining area in the 100 mg/kg- and 400 mg/kg-treated groups compared to the control (e). The western blot analysis of 17 βHSD showed a significant ($p < 0.05$) increased in the 400 mg/kg CPE-treated group compared to the control and 100 mg/kg-treated groups (g, f). Data are expressed as mean ± SEM. Different alphabet letters above the bar graph indicate statistically significant differences between groups.

3.5. Effect of CPE on the Localization of LHR Protein. The immunolocalization of LHR also exhibited a similar trend as we have observed in the 3βHSD. The abundance of LHR was mainly confined to the Leydig cells of mouse testis treated at 400 mg/kg of CPE and 100 mg/kg CPE groups compared to the control group (Figures 6(a)–6(e)).

3.6. Effect of CPE on the Localization and Expression of 17βHSD Protein. The localization of 17βHSD protein exhibited increased abundance in the Leydig cells of mice testis treated at both doses of CPE (100 mg/kg and 400 mg/kg) (Figure 7(a)–7(e)). However, western blot analysis showed a significant ($p < 0.05$) increase of 17βHSD protein in the 400 mg/kg-treated group compared to the control and 100 mg/kg groups (Figures 7(f) and 7(g)).

3.7. Effect of CPE on the Localization and Expression of StAR Protein. Immunolocalization and western blot analyses also showed a significant ($p < 0.05$) increase in the expression of StAR protein in the CPE-treated groups compared to the control (Figures 8(a)–8(g)).

3.8. Effect of CPE on the Localization and Expression of CYP11A1 Protein. The expression of CYP11A1 showed a significant ($p < 0.05$) increase in the expression in the 100 mg/kg CPE-treated group compared to the control; however, a higher dose of CPE showed a mild increase in the CYP11A1 expression compared to the control (Figures 9(a) and 9(b)).

3.9. Effect of CPE on the Localization and Expression of CYP19A1 Protein. Since the docking study showed the
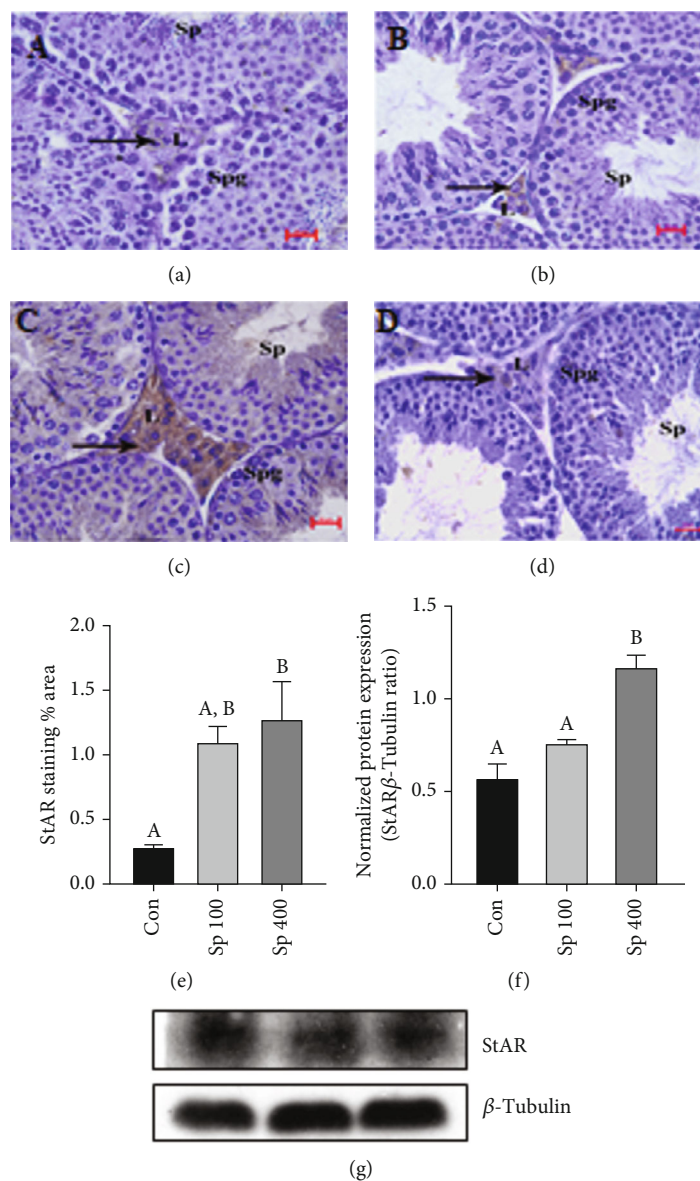
(a)

(b)

(c)

(d)

(e)

(f)

(g)

Figure 8: Localization and expression of StAR in the testis after CPE treatment. The moderate immunostaining of StAR showed in the Leydig cells of 400 mg/kg (c) CPE-treated testis, whereas control and 100 mg/kg group showed mild immunostaining (a, b). The negative control section showed no immunostaining of StAR (d). The quantification StAR stained area showed a significant ($p < 0.05$) increase in the staining area in the 400 mg/kg-treated group compared to the control (e). The western blot analysis of StAR showed a significant ($p < 0.05$) increased in the 400 mg/kg CPE-treated group compared to the control and 100 mg/kg-treated groups (g, f). Data are expressed as mean ± SEM. Different alphabet letters above the bar graph indicate statistically significant differences between groups.

binding of several compounds with CYP19A1, therefore, we have evaluated the expression and localization of the CYP19A1 protein. The immunolocalization study exhibited mild immunostaining of CYP19A1 in the Leydig cells of the control testis, whereas Leydig cells of the testis treated with 100 mg/kg and 400 mg/kg CPE showed strong immunostaining of CYP11A1 (Figures 10(a)–10(d)). Semiquantification of CYP19A1 immunostaining also showed a dose-dependent increase in the abundance (Figure 10(e)). However, western blot analysis exhibited a significant (p<0.05) elevation in the CPY19A1 expression at the higher dose of CPE, compared to the control and lower dose groups (Figures 10(g) and 10(f)).

3.10. Effect of CPE on the Circulating Low-Density Lipoprotein Cholesterol (LDL), High-Density Lipoprotein Cholesterol (HDL), Cholesterol, and Testicular Cholesterol. The treatment of CPE at the dose of 400 mg/kg significantly (p<0.05) lowers the concentration of serum LDL and cholesterol, compared to the control (Figures 11(a) and 11(c)). The circulating HDL was found to be significantly higher ($p < 0.05$) at 400 mg/kg dose compared to the control (Figure 11(b)). The testicular cholesterol concentration was also significantly ($p < 0.05$) elevated in the CPE-treated groups compared to the control (Figure 11(d)).
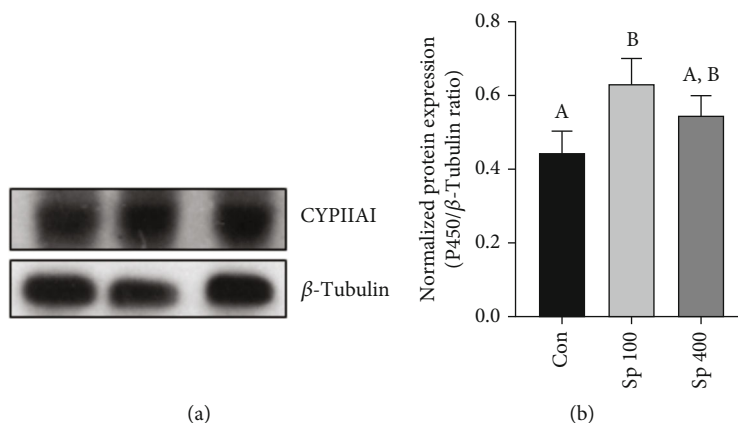
(a)

(b)

FIGURE 9: Expression of CYP11A1 in the testis after CPE treatment. The western blot analysis of CYP11A1 showed a significant ($p < 0.05$) increase in the 400 mg/kg CPE-treated group compared to the control and 100 mg/kg-treated groups (g, f). Data are expressed as mean ± SEM. Different alphabet letters above the bar graph indicate statistically significant differences between groups.

3.11. Effect of CPE on the Circulating Estrogen, Androstenedione, and Testosterone Levels. The circulating estrogen levels exhibited a significant increase in the 400 mg/kg CPE group compared to the control (Figure 12(a)). However, circulating androstenedione was significantly highest in the 100 mg/kg CPE group compared to the other groups (Figure 12(b)). The levels of circulating testosterone decreased in the CPE-treated groups compared to the control (Figure 12(c)).

3.12. Effect of CPE on the Estrogen, Androstenedione, and Testosterone Secretion In Vitro. As our in vivo and in silico results showed a possible modulation of testicular steroidogenesis by the phytochemicals of CPE, therefore, we have also conducted the in vitro study to examine the direct role of CPE on testicular steroidogenesis. The CPE extract at a dose of 10 and 100 μg/ml significantly ($p < 0.05$) elevated estrogen and significantly ($p < 0.05$) decreased androstenedione secretion compared to the control (Figures 13(a) and 13(b)). Only 100 μg/ml dose of CPE increased the testosterone secretion compared to the control (Figure 13(c)).

4. Discussion

The present study has investigated the effect of *Cycas pectinata* seed extract on testicular steroidogenesis by using in vivo and in vitro approaches along with in silico study of its phytochemical constituents' interaction with steroidogenic pathways. *Cycas pectinata* seed has been widely used in some parts of Northeast India for improving male fertility. The use of *Cycas pectinata* seed as a male fertility enhancer has promoted us to evaluate the effects of *Cycas pectinata* seed on testicular steroidogenesis. To the best of our knowledge, the impact of *Cycas pectinata* seed on the steroidogenic pathway has not been investigated yet. The treatment of CPE decreased the levels of testosterone and increased the levels of circulating estrogen. The levels of androstenedione were elevated at a lower dose, not at a higher dose. This discrepancy is not clear from the present study; however, changes in testosterone and estrogen levels by CPE suggest that phytochemicals of CPE might modulate testicular steroidogene-

sis. Whether CPE-mediated testicular steroidogenesis could be positive or negative on the other parameters of testicular activity would require further study. Furthermore, it would be very interesting to examine the effect of CPE on fertility in light of testicular steroidogenesis.

Testicular steroidogenesis uses cholesterol as the substrate for the synthesis of testicular steroid hormones [11, 12]. Therefore, we have investigated the circulating and testicular cholesterol and our results showed that CPE decreased the circulating cholesterol and increased testicular cholesterol. These findings also suggest that the phytochemicals of CPE could modulate testicular steroidogenesis by regulating cholesterol transport. It is also well known that cholesterol is transported to the mitochondria in the steroid-producing tissue and cells by StAR to further conversion [11, 12]. Our results showed that CPE upregulated the expression of testicular StAR, and this finding also suggests that phytochemicals of CPE might regulate the testicular steroidogenesis by stimulating cholesterol in the mitochondria. However, our in silico study has shown the cholesterol antagonist activity of CPE phytocompounds [6]; this discrepancy in the finding could be due to other factors that might be involved in the in vivo conditions. It should also be noted that findings of in silico studies may not be always similar to in vivo conditions. Therefore, further study is required for this discrepancy.

The other marker, CPY11A1, is enzyme responsible for cleaving the side chain of cholesterol and serves as a rate-limiting step of steroid biosynthesis in the testis. The treatment of CPE extracts slightly increased the expression of CYP11A1, the increased expression of CPY11A1 was more pronounced at 100 mg/kg than in high doses. Our in silico study showed that hupehemonoside, pyrrhoxanthinol, pseudojervine, cyclogaleginoside A, cyclopyrroxanthin, pyrrhoxathinol 5,8-furanoide, and 3-didehydro-5-dehydroxyhydratoperidinin showed binding with CYP11A1 and hupehemonoside showed highest binding energy (-10.7 kcal/mol) exhibited three hydrogen bonds with the side chain residues Asn210, Val353, and Gln377. These in vivo and in silico findings suggest that phytochemicals of CPE could act as ligands for CPY11A1 and might have a modulatory role in steroidogenesis. Hupehemonoside has been

(a)   (b)

(c)   (d)

(e)   (f)
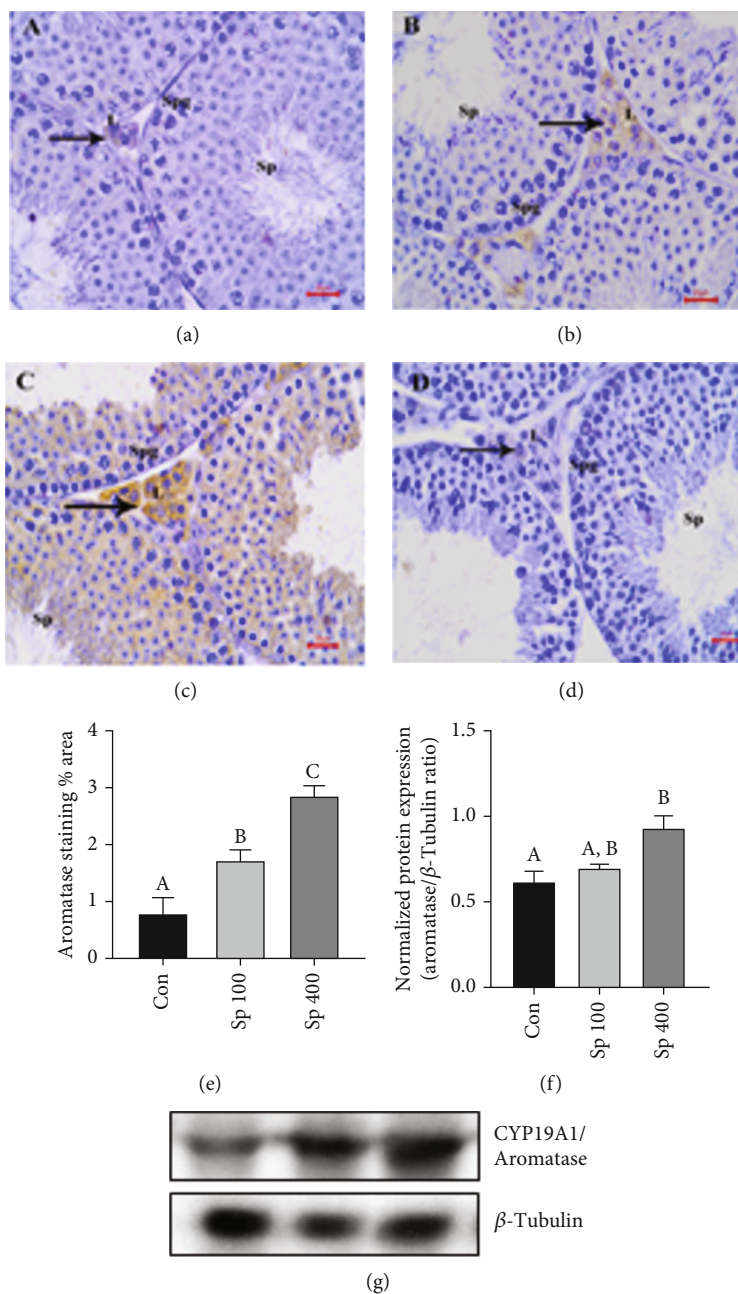
(g)

FIGURE 10: Localization and expression of CYP19A1 in the testis after CPE treatment. The moderate immunostaining of CYP19A1 showed in the Leydig cells of 100 mg/kg (b) and 400 mg/kg (c) CPE-treated testis, whereas control showed mild immunostaining (a). The negative control section showed no immunostaining of CYP19A1 (d). The quantification CYP19A1-stained area showed a dose-dependent significant ($p < 0.05$) increase in the staining area in the CPE-treated groups compared to the control (e). The western blot analysis of CYP19A1 showed a significant ($p < 0.05$) increase in the 400 mg/kg CPE-treated group compared to the control (g, f). Data are expressed as mean ± SEM. Different alphabet letters above the bar graph indicate statistically significant differences between groups.

isolated from other plants such as *Fritillaria ebeiensis* [15], but its functional role has not been widely discussed.

The Leydig cells, the main steroid-producing cell in the testis, mediated testicular steroidogenesis via the binding of LH to LHR [16]. Our immunolocalization study of LHR and 3βHSD also showed the increased abundance of these proteins in the Leydig cells, these findings also suggest a stimulatory role of CPE on testicular steroid biosynthesis. Similarly, CPE also increased the expression of 17βHSD in the testis, with

increased abundance in the Leydig cells. 17βHSD is an important enzyme in testicular steroid biosynthesis, and it is known to convert androstenedione to testosterone [17, 18]. 17βHSD also converts testosterone to androstenedione [19]. Among all the phytochemicals, only hupehemonoside binds well with 17βHSD (-9.3 kcal/mol). A docking study showed that the binding of hupehemonoside is also stabilized by only pi-alkyl and alkyl interactions with the residues Pro187, Met193, Val225, Phe226, and Phe259 in the active site of 17βHSD.
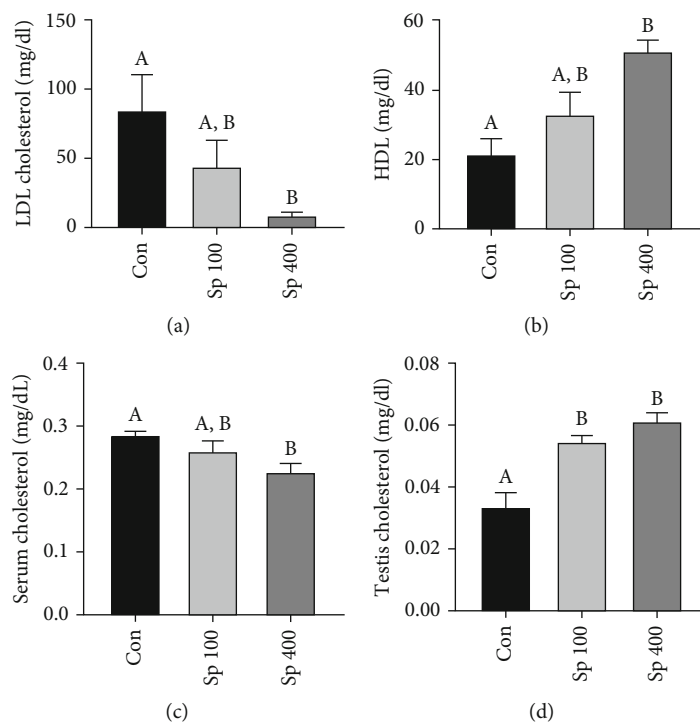
FIGURE 11: The circulating levels of LDL, HDL, serum cholesterol, and testicular cholesterol concentration after CPE treatment. Circulating LDL (a) significantly ($p < 0.05$) decreased and circulating HDL (b) significantly increased in 400 mg/kg-treated group compared to the control and 100 mg/kg-treated groups. The circulating cholesterol also showed a significant ($p < 0.05$) decreased in the 400 mg/kg-treated groups compared to the control (c). The testicular cholesterol concentration showed a significant ($p < 0.05$) increase in the CPE-treated groups compared to the control (d). Data are expressed as mean ± SEM. Different alphabet letters above the bar graph indicate statistically significant differences between groups.
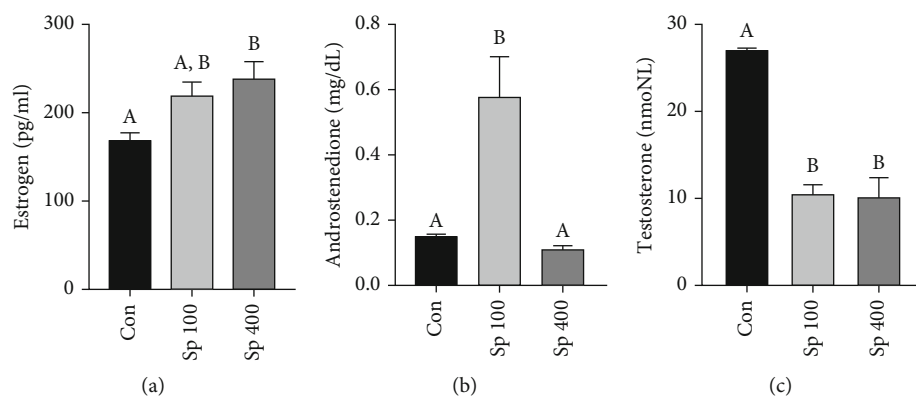

FIGURE 12: The effects of CPE treatment on the circulating estrogen, androstenedione, and testosterone levels. The circulating estrogens showed a significant ($p < 0.05$) increase in the 400 mg/kg-treated groups compared to other groups (a). Androstenedione levels significantly increased in the 100 mg/kg-treated group compared to the other groups (b). Both doses of CPE 100 mg/kg and 400 mg/kg significantly decreased the circulating testosterone compared to the control (c). Data are expressed as mean ± SEM. Different alphabet letters above the bar graph indicate statistically significant differences between groups.

Furthermore, the decreased circulating testosterone and slightly increased circulating estrogen levels suggest that testosterone might have been converted to estrogen by aromatase (CYP19A1). CYP19A1 is expressed in the Leydig cells and aromatizes testosterone to estrogen [20, 21]. Our immunolocalization and western blot study also showed CPE increases the testicular CYP19A1 expression with abundance in the Leydig cells. Furthermore, decreased testosterone and mildly elevated estrogen levels in the CPE-treated groups could be explained by increased expression of CYP19A1 (aromatase) by CPE phytocompounds. These findings further strengthen the concept of the aromatization of testosterone to estrogen by phytochemical constituents of CPE.

The increased estrogen decreased testosterone along with increased aromatase expression has prompted us to analyze the binding of phytochemicals to the CYP19A1. The
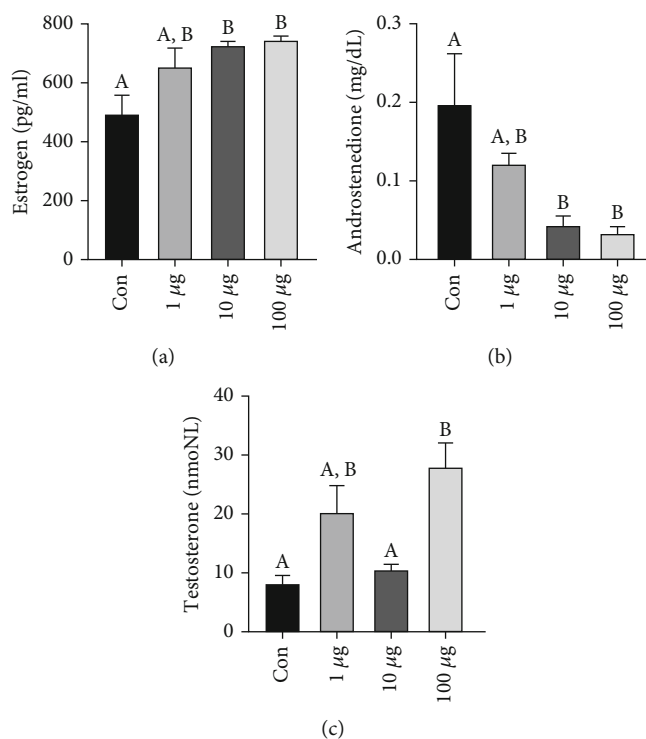
(a)

(b)

(c)

Figure 13: The *in vitro* effects of CPE treatment on the estrogen, androstenedione, and testosterone secretion. Estrogen (a) secretion was significantly ($p < 0.05$) increased in $10\,\mu$g/ml and $100\,\mu$g/ml whereas, androstenedione (b) secretion was significantly decreased in the $10\,\mu$g/ml- and $100\,\mu$g/ml-treated groups compared to the control. Furthermore, testosterone (c) secretion was elevated only at the $100\,\mu$g/ml-treated group. Different alphabet letters above the bar graph indicate statistically significant differences between groups.

phytochemicals, 3-didehydro-5-dehydroxyhydratoperidinin, 6-epiheteroxanthin, astaxanthin, auroxanthin, corbiculaxanthin, cucurbitaxanthin A, cycloviolaxanthin, halocynthiaxanthin, ipomoeaxanthin A, mactraxanthin, pyrrhoxanthinol, and pyrrhoxathinol 5,8-furanoide, binds with CYP19A1 with the binding energy of -10.1, -8.7, -9.9, -8.2, -9.8, -9.2, -8.3, -9.3, -9.3, -9.5, -9.7, and -9.2 kcal/mol, respectively. Furthermore, these phytochemicals do not exhibit stacking interactions such as π-π, π-anion, and π-σ interactions due to the nonaromaticity of their structures, except pyrrhoxathinol-5, 8-furanoide where amide-π stacking was observed with furanoide ring. The compound with the highest binding affinity, i.e., 3-didehydro-5-dehydroxyhydratoperidinin exhibited two hydrogen bonds with the side chain residues Cys437 and Ala438. Further, the π-alkyl and alkyl interactions with the residues Ile132, Ile133, Phe134, Phe138, Leu152, Phe221, Val370, and Val373 greatly contributed to its stability in the active site. Astaxanthin with a binding affinity of -9.9 kcal/mol exhibited the highest number of hydrogen bond interactions with four side-chain residues Arg115, Arg145, Thr310, and Ser314. It is also stabilized by the π-alkyl and alkyl interactions with the residues Ile133, Trp224, Ala306, Met364, Val369, Val370, Phe430, Cys437, and Ala438. Auroxanthin exhibited two hydrogen bonds with the residues Ala438 and Gly439. Corbiculaxanthin is oriented in such a way that it established two hydrogen bonds with the residues Arg145 and Thr310. Ipomoeaxanthin A also exhibited two hydrogen bonds with the residues Ser314 and Cys437. Halocynthiaxanthin and mactraxanthin exhibited

one hydrogen bond interaction each with the residues Ala306 and Cys437, respectively. Although 6-epiheteroxanthin, cucurbitaxanthin A, and cycloviolaxanthin are highly stabilized in their binding cavity, they do not establish any hydrogen bond interactions. Their stability comes predominantly from hydrophobic alkyl and π-alkyl interactions.

As we have previously reported the 32 major phytochemicals, out of which 12 phytochemicals showed binding with CYP19A1; however, with CYP11A1 and 17βHSD only, a few phytochemicals showed binding. This in silico and *in vivo* data clearly showed that CPE phytochemicals have more ligands for CYP19A1. To analyze the direct effects of CPE phytochemicals, we have performed an *in vitro* study. The results of *in vitro* study showed that the highest dose of CPE increase testosterone; however, in our *in vivo* study, the levels of testosterone were decreased. The reason for this discrepancy would be factors present *in vitro* and *in vivo* conditions are not the same. The increased estrogen secretion in the *in vitro* study also suggests that CPE phytochemicals could be involved in the conversion of testosterone to estrogen because CPE phytochemicals might modulate the CYP19A1 expression as we have shown in the *in vivo* study. However, it should be noted that the levels of androstenedione were decreased with CPE treatment, along with an increase in estrogen secretion. These findings suggest that CPE could modulate the activity of 17βHSD and CYP19A1, thereby regulating the testicular steroid biosynthesis.

5. Conclusions

This is the first report on the effects of CPE phytochemicals on testicular steroid biosynthesis by *in vivo*, *in vitro*, and in silico approaches. Furthermore, it might be suggested that CPE could regulate testicular activity via the modulation of estrogen and testosterone. The positive or negative impacts of CPE-mediated testicular steroidogenesis on fertility would be important to unravel the role of CPE on male reproduction. This study also opens a future avenue to use the identified compounds for the modulation of testicular steroidogenesis in different conditions.

Data Availability

The data used to support the study's conclusions are included in the paper.

Conflicts of Interest

The authors declare no conflicts of interest.

Authors' Contributions

VKR, CM, and GG contributed to the conceptualization and design of the study. VKR and CM contributed to the execution of experimental procedures and data collection. BM and VPS performed all the docking experiments and analyzed the data. VKR, CM, BM, VPS, and GG contributed to the analysis of data, discussion, and manuscript preparation.

Acknowledgments

References

[1] H. P. Verma and S. K. Singh, "Effect of aqueous leaf extract of Dalbergia sissoo Roxb. on spermatogenesis and fertility in male mice," *The European Journal of Contraception & Reproductive Health Care*, vol. 19, no. 6, p. 475, 2014.

[2] A. L. Demain and S. Sanchez, "Microbial drug discovery: 80 years of progress," *The Journal of Antibiotics*, vol. 62, no. 1, pp. 5–16, 2009.

[3] J. S. Khuraijam and R. Singh, "Ethnobotany of Cycas pectinata Ham," *Northeast India Encephalartos*, vol. 119, pp. 18–23, 2015.

[4] S. Laishram, Y. Sheikh, D. S. Moirangthem et al., "Anti-diabetic molecules from *Cycas pectinata* Griff. traditionally used by the Maiba-Maibi," *Phytomedicine*, vol. 22, no. 1, pp. 23–26, 2015.

[5] A. M. Tareq, S. Farhad, A. N. Uddin et al., "Chemical profiles, pharmacological properties, and *in silico* studies provide new insights on *Cycas pectinata*," *Heliyon*, vol. 6, no. 6, article e04061, 2020.

[6] C. C. Marak, B. N. Marak, V. P. Singh, G. Gurusubramanian, and V. K. Roy, "Phytochemical analysis, in silico study and toxicity profile of *Cycas pectinata* Buch.-Ham seed in mice," *Drug and Chemical Toxicology*, vol. 46, no. 2, pp. 330–342, 2023.

[7] B. R. Zirkin and H. Chen, "Regulation of Leydig cell steroidogenic function during aging," *Biology of Reproduction*, vol. 63, no. 4, pp. 977–981, 2000.

[8] B. R. Zirkin and V. Papadopoulos, "Leydig cells: formation, function, and regulation," *Biology of Reproduction*, vol. 99, no. 1, pp. 101–111, 2018.

[9] A. H. Payne and D. B. Hales, "Overview of steroidogenic enzymes in the pathway from cholesterol to active steroid hormones," *Endocrine Reviews*, vol. 25, no. 6, pp. 947–970, 2004.

[10] S. Carreau, "Leydig cell aromatase," in *The Leydig Cell in Health and Disease*, A. H. Payne and M. P. Hardy, Eds., pp. 189–195, Humana Press, 2007.

[11] A. H. Payne and G. L. Youngblood, "Regulation of expression of steroidogenic enzymes in Leydig cells," *Biology of Reproduction*, vol. 52, no. 2, pp. 217–225, 1995.

[12] S. A. Andric and T. S. Kostic, "Regulation of Leydig cell steroidogenesis: intriguing network of signaling pathways and mitochondrial signalosome," *Current Opinion in Endocrine and Metabolic Research*, vol. 6, pp. 7–20, 2019.

[13] E. C. Jensen, "Quantitative analysis of histological staining and fluorescence using ImageJ," *The Anatomical Record*, vol. 296, no. 3, pp. 378–381, 2013.

[14] M. Jeremy, G. Gurusubramanian, and V. K. Roy, "Vitamin D3 mediated regulation of steroidogenesis mitigates testicular activity in an aged rat model," *The Journal of Steroid Biochemistry and Molecular Biology*, vol. 190, pp. 64–75, 2019.

[15] J. Z. Wu, X. P. Pan, M. A. Lou, X. S. Wang, and D. K. Ling, "Studies on the chemical constituents of Fritillaria in Hubei. X. Isolation and identification of alkaloids from Fritillaria ebeiensis var. purpurea GD Yu et P. Li," *Yao xue xue bao = Acta Pharmaceutica Sinica*, vol. 24, no. 8, pp. 600–605, 1989.

[16] T. Pakarainen, F. P. Zhang, S. Mäkelä, M. Poutanen, and I. Huhtaniemi, "Testosterone replacement therapy induces spermatogenesis and partially restores fertility in luteinizing hormone receptor knockout mice," *Endocrinology*, vol. 146, no. 2, pp. 596–606, 2005.

[17] P. J. O'Shaughnessy, P. J. Baker, M. Heikkila, S. Vainio, and A. P. McMahon, "Localization of 17β-hydroxysteroid dehydrogenase/17-ketosteroid reductase isoform expression in the developing mouse testis—androstenedione is the major androgen secreted by fetal/neonatal Leydig cells," *Endocrinology*, vol. 141, no. 7, pp. 2631–2637, 2000.

[18] E. Sagsak, Z. Aycan, S. Savas-Erdeve, M. Keskin, S. Cetinkaya, and K. Karaer, "17βHSD-3 enzyme deficiency due to novel mutations in the HSD17B3 gene diagnosed in a neonate," *Journal of Pediatric Endocrinology & Metabolism*, vol. 28, no. 7-8, pp. 957–959, 2015.

[19] N. Khan-Sabir and R. J. Auchus, "Human 17βHSD type 2 reversibly interconverts androgens and estrogens at equal rates in vivo," *Fertility and Sterility*, vol. 78, p. S281, 2002.

[20] J. D. Chow, E. R. Simpson, and W. C. Boon, "Alternative 5$'$-untranslated first exons of the mouse Cyp19A1 (aromatase) gene," *The Journal of Steroid Biochemistry and Molecular Biology*, vol. 115, no. 3-5, pp. 115–125, 2009.

[21] S. Bourguiba, C. Genissel, S. Lambard, H. Bouraïma, and S. Carreau, "Regulation of aromatase gene expression in Leydig cells and germ cells," *The Journal of Steroid Biochemistry and Molecular Biology*, vol. 86, no. 3-5, pp. 335–343, 2003.